Characterization of Finite-Ground CPW Reactive Series-Connected Elements for Innovative Design of Uniplanar M(H)MICs

Lei Zhu, *Senior Member, IEEE,* and Ke Wu, *Fellow, IEEE*

***Abstract*—In this paper, a variety of finite-ground coplanar waveguide (FGCPW) reactive series-connected capacitive and inductive elements are extensively studied and characterized as equivalent-circuit models that include complex parasitic effects caused by finite-ground widths. These models are developed by implementing a numerical calibration procedure called short-open calibration, which is used to extract characteristic parameters of the circuit model from full-wave method-of-moments calculations. The proposed model is generally described as an equivalent series admittance (Y_g) or impedance (Z_g) together with a pair of shunt admittances (Y_p) for FGCPW series-connected structures. With the new scheme, the FGCPW elements of interest behave like lossless lumped elements at low-frequency range, consisting of a series capacitance or inductance, as well as two shunt capacitances. As frequency increases, however, Y_g and Z_g exhibit a frequency-related dispersion and also a lossy resonance behavior, which stand for some added inductive or capacitive coupling effect caused by the extent of finite-ground width. On the other hand, unbounded radiation effect, considered in this model, appears too strong to be ignored around resonance. Theoretical and experimental results that are compared very well with each other are shown for interesting electrical behaviors of finite-ground structures. An innovative uniplanar three-stage bandstop filter is designed and measured on the basis of its simplified equivalent-circuit model.**

***Index Terms*—CAD, circuit model, finite-ground coplanar waveguide, method of moments, series reactance, short-open calibration, uniplanar filter.**

I. Introduction

COPLANAR waveguides (CPWs) have found a wide range of applications in the design of uniplanar monolithic microwave integrated circuits (MMICs) including multilayered geometry because of its attractive features such as low-frequency dispersion, easy insertion of shunt and series active devices, and less substrate dependence [1]. However, the prototype CPW structure still has some contestable problems in the design of high-density MMICs, namely, potentially an excessive number of via holes or multilayered arrangement of substrate to eliminate potential parasitic effects of surface waves or parallel-plate modes, leaky-wave loss, as well as unwanted coupled slot line modes. They may be related to electrically large or infinitely extended ground planes. On the other hand, the CPW structure always has finite-width ground planes in practice, which are, in most cases, electrically sensitive. Therefore, ignoring the effects of the ground plane in the design may lead to erroneous results at high frequencies. Interestingly, such parasitic effects may, in most cases, turn out to be very useful if they can be well understood and precisely characterized. In addition, an adequate choice of finite ground planes (or strips) provides us with an additional degree of design freedom, not only in overcoming these problems, but also in leading to size-miniaturized and low-loss CPW circuits [2]–[6].

Accordingly, the finite-ground coplanar waveguide (FGCPW) has been gaining much attention in the design of a variety of high-quality uniplanar active/passive circuits and antennas, in conjunction with other uniplanar transmission lines such as the coplanar stripline (CPS). In the past years, a large amount of research has been oriented toward accurate characterization of open or shielded CPW discontinuities by using a full-wave method of moments (MoM), e.g., [7], [8]. Very limited works to date have been carried out for accurate modeling of FGCPW discontinuities or circuit blocks. In [5], a finite-difference time-domain (FDTD) algorithm was applied for designing some FGCPW circuit elements on the basis of a trial-and-error procedure. In [6], an experimental investigation was made for parametric extraction of equivalent-circuit models for FGCPW open- and short-circuit terminated series stubs. Nevertheless, it requires much effort to develop a reliable and versatile technique for characterization of a variety of FGCPW circuit elements. This issue is of paramount importance in accurate design and effective realization of FGCPW integrated circuits and antennas. Such design models should be able to account for frequency dispersion, physical radiation/leakage effects, and parasitic capacitive and/or inductive factors, to benefit or alleviate parasitic effects in the design of uniplanar circuits or antennas with designated electrical performance.

In this paper, our effort is focused on a full-wave characterization of two classes of FGCPW reactive series-connected elements. A special parametric-extraction technique is developed from field results for equivalent-circuit modeling, as well as physical understanding of electrical behavior. This is realized by applying our newly proposed numerical deembedding technique called short-open calibration (SOC) [9]–[11], [12], [13] to calibrate (deembed) the calculated parameters based on our deterministic full-wave MoM [14]. The equivalent-circuit model proposed in this paper consists of one series impedance

Manuscript received April 7, 1999. This work was supported by the Natural Sciences and Engineering Research Council of Canada.

L. Zhu was with the Department of Electrical and Computer Engineering, École Polytechnique de Montréal, Montréal, QC, Canada H3V 1A2. He is now with the School of Electrical and Electronic Engineering, Nanyang Technological University, Singapore 939798 (e-mail: EZhuL@ntu.edu.sg).

K. Wu is with the Poly-Grames Research Center, Département de Génie Électrique, École Polytechnique de Montréal, Montréal, QC, Canada H3V 1A2 (e-mail: wuke@grmes.polymtl.ca).

Publisher Item Identifier S 0018-9480(02)01165-1.

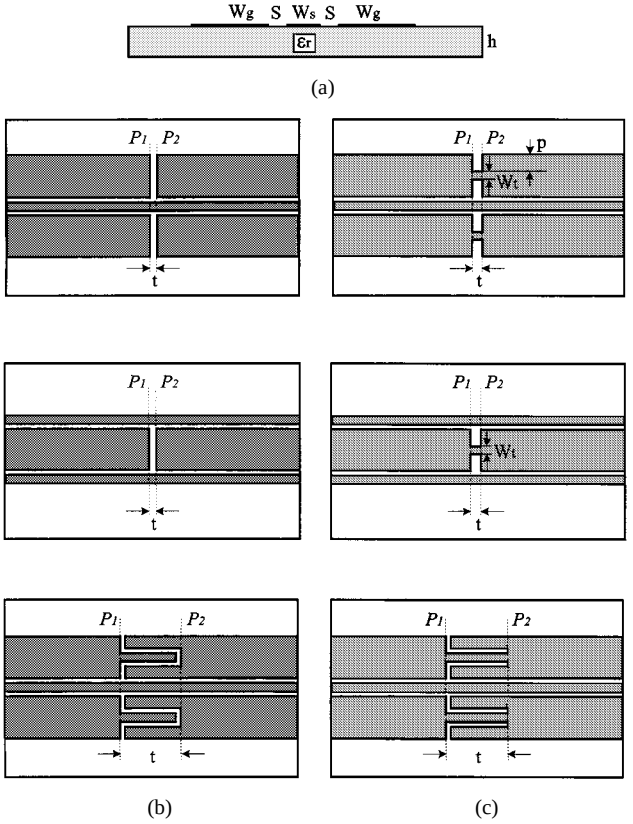

Fig. 1. Layout view of FGCPW reactive series-connected elements. (a) Cross section of FGCPW line. (b) Capacitive series element. (c) Inductive series element.

or admittance, as well as a pair of two shunt reactances. The obtained electrical parameters exhibit lossless lumped-element behaviors at low frequency and upgrades to lossy distributed-element behaviors as frequency increases. Calculated characteristic curves are provided to reveal interesting electrical performance. In addition, experiments are made to verify our proposed circuit model. A uniplanar three-stage bandstop filter is also designed on the basis of its extracted and simplified equivalent circuit scheme and it is measured to compare its predicted frequency response.

II. Formulation of Unified Circuit Model

Fig. 1(a) depicts the cross section of an FGCPW line without backside grounding, where its two finitely extended ground planes (W_g) are located adjacently to its central strip conductor (W_s). Fig. 1(b) and (c) shows a schematic layout of two classes of the FGCPW reactive series-connected elements to be studied. As opposed to their conventional CPW structures [1], the FGCPW elements have an additional degree of design freedom for the realization of a predesignated series reactance in uniplanar circuits. With the finite extent of the two ground planes, those FGCPW elements can be designed by splitting longitudinally the ground planes of the uniform FGCPW line to make up a gap structure or cutting (notching) them transversely to form a narrow line section, as described in the top figures of Fig. 1(b) and (c). Of course, the series reactance elements can also be realized by applying this scheme to the signal strip with finite width, as indicated in the central figures of Fig. 1(b) and (c). Otherwise, Fig. 1(b) and (c) presents two alternative FGCPW structures that potentially have large series capacitance or inductance, realized by constituting the open- or short-circuit terminated series stub sections, as in [6]. In the following, we will make a detailed description on the development of an equivalent model-oriented parametric-extraction technique from our full-wave MoM-based field calculations. This procedure calls for our SOC technique, which allows for efficient network-oriented optimization of FGCPW-based uniplanar circuits, and also for gaining physical insight into high-frequency electrical properties of physical layout of the circuits.

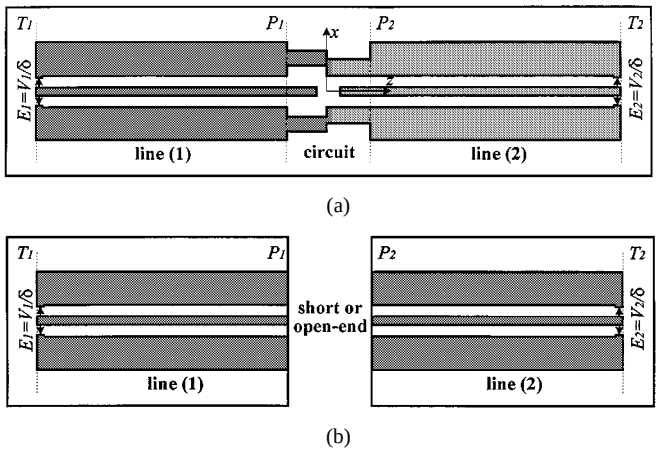

Fig. 2. Physical description for the parametric extraction of FGCPW discontinuity by applying our SOC scheme in a full-wave MoM. (a) Generalized FGCPW discontinuity. (b) Calibration standards: short and open elements.

A. Full-Wave MoM Algorithm

A full-wave MoM algorithm [14] is extended here for the full-wave characterization of a generalized two-port FGCPW discontinuity on an unbounded dielectric substrate with finite thickness. Fig. 2(a) depicts its physical layout for the deterministic MoM field calculations of its electric parameters at two ports that are usually located far away from the region (P_1–P_2) of discontinuity. The two selected ports, namely, T_1 and T_2, are simultaneously driven by a pair of impressed electric fields across the transversely infinitesimal interval (δ) between the signal strip and two ground planes (strips), as shown in Fig. 2(a). The entire FGCPW discontinuity is classified into two distinct regions: external lines (T_1–P_1) and (T_2–P_2) along which the input/output signals propagate and circuit discontinuity (P_1–P_2) to which all the discontinuity effects are attributed. Following the MoM analytical procedure, an electric-field integral equation (EFIE) governing the total current density can be established over the conductor surface

$$\sum_{i=1}^{2}\left[\vec{E}_i^{\text{inc}}+\int_{\text{line}(i)}\left(\overline{\overline{G}}\cdot\vec{J}_i\right)dS\right]+\int_{\text{circuit}}\left(\overline{\overline{G}}\cdot\vec{J}_c\right)dS=0 \tag{1}$$

where $\overline{\overline{G}}$ denotes a dyadic Green's function for the layered structure. $\vec{J}_i$ and $\vec{J}_c$ are the current densities over the signal and ground strips of the ith FGCPW line ($i=1$, and the FGCPW

circuit discontinuity, respectively. $\vec{E}_i^{\text{inc}}$ denotes the so-called excitation source in the deterministic MoM formulation [14] and it is represented here as a pair of impressed voltages having reverse orientation and identical magnitude at the ports of each FGCPW line, i.e., for the ith line

$$\vec{E}_i^{\text{inc}} = \begin{cases} +\vec{x}V_i/\delta, & W_s/2 \le x \le W_s/2+\delta \\ -\vec{x}V_i/\delta, & -W_s/2-\delta \le x \le -W_s/2 \\ 0, & \text{elsewhere} \end{cases} \tag{2}$$

in which δ represents the transversely infinitesimal interval at each port, across which the impressed voltage V_i is introduced. By applying the Galerkin's technique into (2), a source-type matrix equation is derived, allowing for the calculation of $\vec{J}_i$ and $\vec{J}_c$. By classifying further the external line region into the port terminal (t) and uniform FGCPW line section (l), such a matrix equation can be formulated in terms of impedance, voltage, and current sub-matrices as follows:

$$\begin{bmatrix} Z^{tt} & Z^{tl} & 0 \\ Z^{lt} & Z^{ll} & Z^{lc} \\ 0 & Z^{cl} & Z^{cc} \end{bmatrix} \cdot \begin{bmatrix} I^t \\ I^l \\ I^c \end{bmatrix} = \begin{bmatrix} V^t \\ 0 \\ 0 \end{bmatrix}. \tag{3}$$

Here, V^t and I^i are column voltage and current sub-matrices standing for the impressed voltages and their corresponding current responses at the ith port, while $Z^{ij}(i, j = t, l, c)$ denotes an impedance sub-matrice that describes the field interaction between the two regions (i and j). As such, the Z- or Y-matrix network defined at the two ports can be deduced with the explicit interrelation between the port voltages and currents, namely, V_i and I_i ($i = 1, 2$).

B. SOC Procedure

Now, let us look at the parametric —extraction scheme, which is the key aspect in developing the equivalent-circuit model or network for a specific physical layout from the above MoM-based field calculations. A numerical calibration (deembedding) technique, i.e., SOC [9], is applied to extract (deembed) the circuit model (network) by removing all the possible numerical error terms including numerical noise, which exist in the deterministic three-dimensional (3-D) MoM scheme. These terms, which are related to the field model, are brought by the approximation of source mechanism [10] and inconsistency between the two-dimensional (2-D) and 3-D MoM definition of a uniform line section [11], [12], [13]. This is because it is impossible to analytically formulate the impressed source for a layered geometry, and its numerical representation is always approximate in nature. Usually, the accuracy of the numerical model is not consistent with frequency, discretization, and other model parameters (e.g., the finite number of basis functions). Potential error effects may be significant as compared to the extracted circuit parameters if the direct field-circuit parameters conversion is used, which involve both 2-D and 3-D concepts and are not necessarily consistent for particular electrical parameters such as characteristic impedance. This causes additional troubles in the parameter-extraction procedure.

To remove such hurdles, we have developed this SOC technique, which was inspired from the well-developed calibration procedures such as thru-reflect line (TRL), e.g., [15]–[17], in microwave measurements. One of the most noted features in this new scheme is to be free from the use of characteristic impedance of a uniform line, which is a usually quarreling issue [11], [12], [13]. Compared to the TRL technique for measurements, our SOC technique requires only two calibration elements in the whole numerical extracting or deembedding procedure, namely, short and open circuits.

Fig. 2(b) depicts the physical layout of such two FGCPW elements for the purpose of numerical calibration with respect to Fig. 2(a). As shown in Fig. 2(b), the impressed voltages drive the ports (T_i) of reference and the other sides (P_i) feature perfect electric or magnetic walls, thereby exhibiting an ideal FGCPW short or open end for the circuit representation. They are then characterized by our above-discussed MoM scheme to evaluate and extract electric behavior of the error terms incurred in related line sections (T_1–P_1) and (T_2–P_2) of the two-port FGCPW discontinuity, as described in Fig. 2(a). A pair of EFIEs that correspond to the short and open standards are represented by

$$\begin{cases} \vec{E}_{is}^{\text{inc}} + \displaystyle\int_{\text{line}(i)} \left(\overline{\overline{G}} - \overline{\overline{G}}'\right) \cdot \vec{J}_{is}\, dS = 0 & \text{(short-circuit)} \\ \vec{E}_{io}^{\text{inc}} + \displaystyle\int_{\text{line}(i)} \left(\overline{\overline{G}} + \overline{\overline{G}}'\right) \cdot \vec{J}_{io}\, dS = 0 & \text{(open-circuit)} \end{cases} \tag{4}$$

in which $\overline{\overline{G}}'$ denotes the image counterpart of $\overline{\overline{G}}$ with respect to the terminal [$P_i\,(i = 1, 2)$ in Fig. 2(a)] P_i for the ith FGCPW standard line and relevant electric or magnetic wall. Upon the MoM calculation of current density over the entire conductor surface of this line, a circuit matrix in relation to the error terms can analytically be deduced through the solution of three voltage–current equations for the short and open and the additional condition related to the network reciprocity, as detailed in [9]. By normalizing the port electric currents of the short and open circuits, as well as the current flowing at the short, namely, I_{is}^t, I_{io}^t, and I_{is}^p, to their respective port voltages, V_{is}^t and V_{io}^t, the error terms for the ith line can be written by the following $ABCD$ matrix:

$$[X_i] = \begin{bmatrix} \overline{I}_{is}^t/\overline{I}_{is}^p & -1/\overline{I}_{is}^p \\ -\overline{I}_{is}^p\overline{I}_{io}^t/(\overline{I}_{is}^t - \overline{I}_{io}^t) & \overline{I}_{is}^p/(\overline{I}_{is}^t - \overline{I}_{io}^t) \end{bmatrix} \tag{5}$$

in which $\overline{I}_{is}^t$, $\overline{I}_{io}^t$, and $\overline{I}_{is}^p$ are the three normalized currents. By applying (5) to calibrate (or correct) the parameters obtained from the solution of (3), the electric behavior of the two-port FGCPW discontinuity in question can accurately be characterized into an equivalent admittance- or impedance-matrix circuit model at the two chosen references P_1 and P_2. This model considers, as far as the MoM calculations permit, all the physical effects in connection with the FGCPW circuit region of interest including effects of high-order modes generated at the interface between the FGCPW line and core discontinuity region.

III. Results and Design Examples

In this section, the SOC scheme is applied to the accurate parametric extraction of the complete circuit model from our full-wave MoM-based calculations for two classes of the FGCPW reactive series-connected elements, as described in

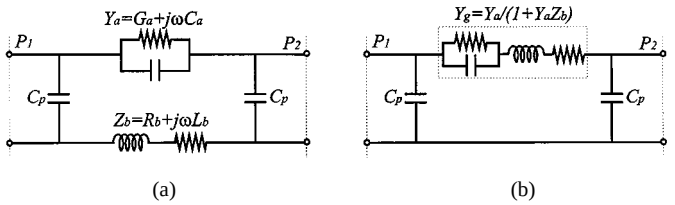

(a) (b)

Fig. 3. Computer-aided design (CAD)-oriented unified model of FGCPW capacitive series-connected elements, as shown in Fig. 1(b). (a) Initial circuit model. (b) Modified circuit model.

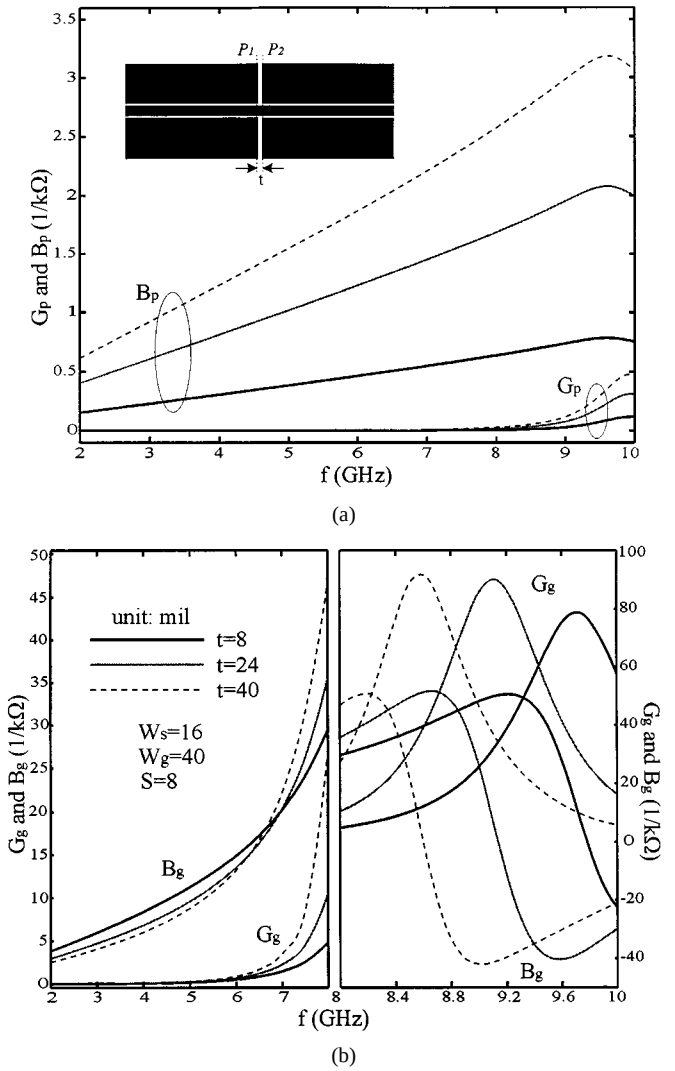

Fig. 4. Calibrated (or extracted) equivalent-circuit parameters of wide-ground FGCPW capacitive series-connected elements. (a) Shunt admittance $Y_p = G_p + jB_p$. (b) Series admittance $Y_g = G_g + jB_g$.

Fig. 1(b) and (c). In addition, our own experiments are carried out to verify the accuracy of our proposed equivalent-circuit model or network. Finally, an innovative uniplanar three-stage FGCPW bandstop filter is designed with the developed circuit model and then a filter sample is fabricated and measured to compare with the predicted results.

A. FGCPW Series Capacitance Elements

Fig. 3(a) depicts the initial circuit model for FGCPW series-connected (gap) capacitive structures, as in Fig. 1(b), which consists of two shunt capacitors (C_p) and a pair of parallel capac-

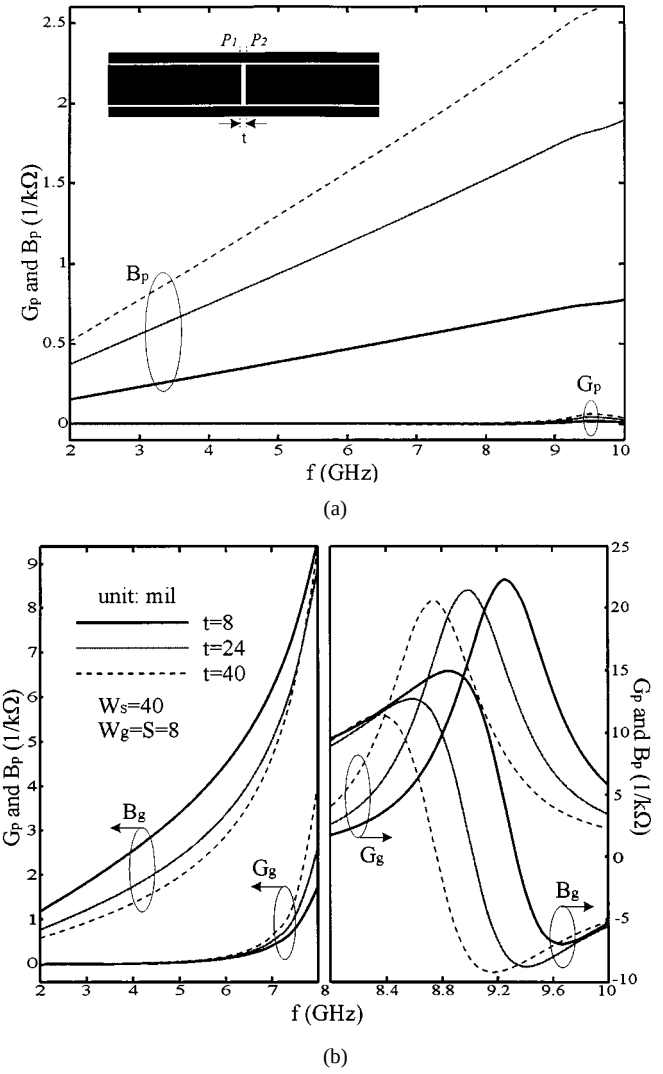

Fig. 5. Frequency response of the calibrated lumped-circuit parameters of wide-strip FGCPW capacitive series-connected elements as a function of the gap interval. (a) Shunt admittance $Y_p = G_p + jB_p$. (b) Series admittance $Y_g = G_g + jB_g$.

itive admittance ($Y_a = Ga + j\omega C_a$) and inductive impedance ($Z_b = R_b + j\omega L_b$) at the two reference planes P_1 and P_2. Such a circuit topology is different from that of a microstrip or CPW gap structure, which has electrically infinite extended ground planes. In this case, Z_b represents an additional inductive parameter caused by the finite extent of signal- or ground-strip widths if the other strip is gap discontinued. Further, this original model can be converted into its more convenient format, as shown in Fig. 3(b), where the capacitive Y_a and inductive Z_b are put together to make up a series lossy *RLC* resonator sandwiched between the two FGCPW open ends. The loss factor is related to a potential radiation generated by electric field distributed inside the gap region and also current density flowing along the continuous signal- or ground-line section.

Special attention is paid to the modeling characterization of two FGCPW structures that have wide ground-strip gap and wide signal-strip gap. They are usually responsible for significant coupling strength and serious resonant behavior. Figs. 4 and 5 give a set of SOC-calibrated frequency-dependent lumped elements of the described circuit model. To highlight

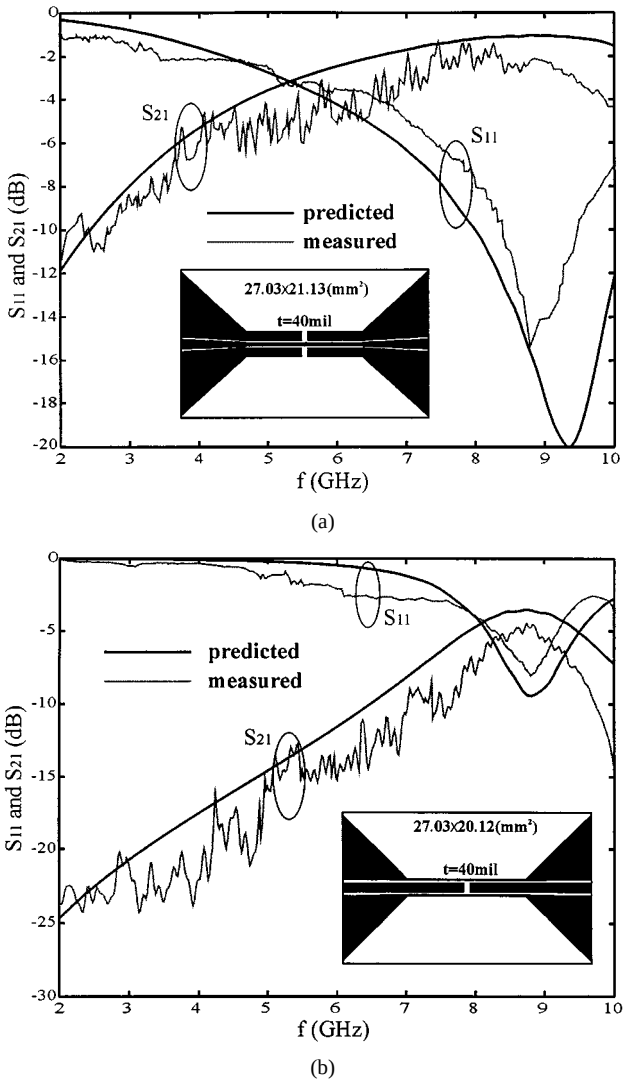

Fig. 6. Predicted and measured results for the two FGCPW capacitive series-connected structures, as discussed in Figs. 5 and 6, which are attached with two tapered 50-Ω CPW line sections at the terminals for facilitating measurements. (a) Frequency response for a wide ground-strip gap. (b) Frequency response for a wide signal-strip gap.

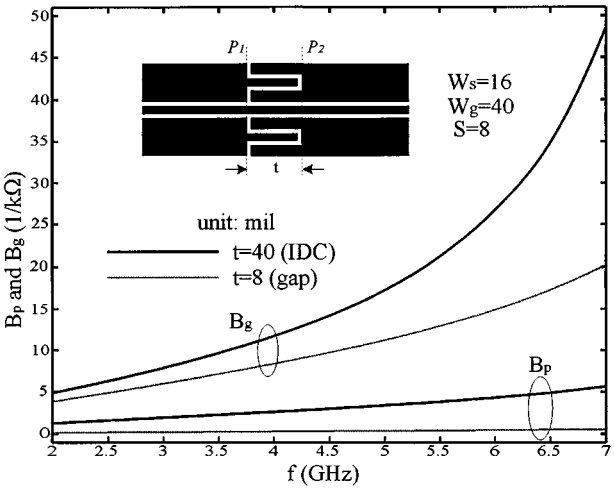

Fig. 7. Dispersion properties of accurately extracted shunt and series susceptances (B_p and B_g) of FGCPW IDC structures compared to those of an FGCPW gap ($t = 8$ mil), as depicted in Fig. 4.

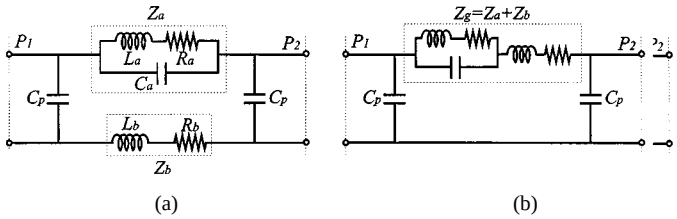

Fig. 8. Proposed CAD-oriented unified circuit model of an FGCPW inductive series-connected element, as shown in Fig. 1(c). (a) Initial circuit model. (b) Modified circuit model.

resonance characteristics at high frequency, the complete curves for $Y_g(= G_g + jB_g)$ are plotted over the two differently scaled frequency ranges (2.0–8.0 GHz) and (8.0–10.0 GHz), as shown in Figs. 4(b) and 5(b). Generally, the two extracted shunt capacitances (C_p) are found to be virtually frequency independent within the noted frequency range (2.0–10.0 GHz), while they are negligible over the frequency range of interest in the circuit model.

On the other hand, Figs. 4(b) and 5(b) indicate that the series susceptance (B_g) behaves quasi-linearly in the low-frequency range and then an abrupt increment occurs as frequency increases further. The series conductance (G_g) is extremely small at low frequency and then it goes up rapidly. As frequency increases further, B_g drops quickly while G_g is raised to a certain maximum value, thus suggesting the existence of an *RLC* resonance phenomenon. If the gap distance (t) becomes shortened, B_g is slightly shifted up at low frequency, thereby showing that the capacitive coupling gains a great enhancement. Nevertheless, the resonant frequency appears to move downward, which indicates a significant increase of the series inductance (L_b) and the series capacitance may remain intact (C_a). To our knowledge, this is mainly influenced by the inductive (signal or ground) stripline section with a narrow width around the air–gap region.

To verify our proposed model and the above-discussed properties, two FGCPW gap structures are fabricated and measured. They are realized with $t = 24$ mil with tapered 50-Ω CPW lines at the two sides of the circuit that facilitates measurements with our network analyzer. Predicted return and insertion losses obtained from the extracted network are plotted together with the measured results in Fig. 6, showing a good agreement. Furthermore, they are to confirm very well our claimed existence of the "resonance" behavior at high frequency. In fact, radiation loss around the resonant frequency is too significant to be ignored in the extracted circuit model. Given that gap distance $t = 24$ mil, the insertion loss (S_{21}) in Fig. 6(a) is found much higher than that in Fig. 6(b), which indicates a large enhancement of capacitive coupling by using an FGCPW wide ground-strip gap. This coupling behavior can easily be understood by comparing two groups of our SOC-extracted series susceptance (B_g), as shown in Figs. 5(b) and 6(b).

Fig. 7 depicts frequency response of the SOC-calibrated susceptances (B_g and B_p) of alternative FGCPW capacitive series-connected element together with that of the gap structure in Fig. 4. Here, a pair of interdigital capacitor (IDC) structures are arranged on the two ground strips to enhance further the coupling strength. The extracted B_g and B_p appear to increase

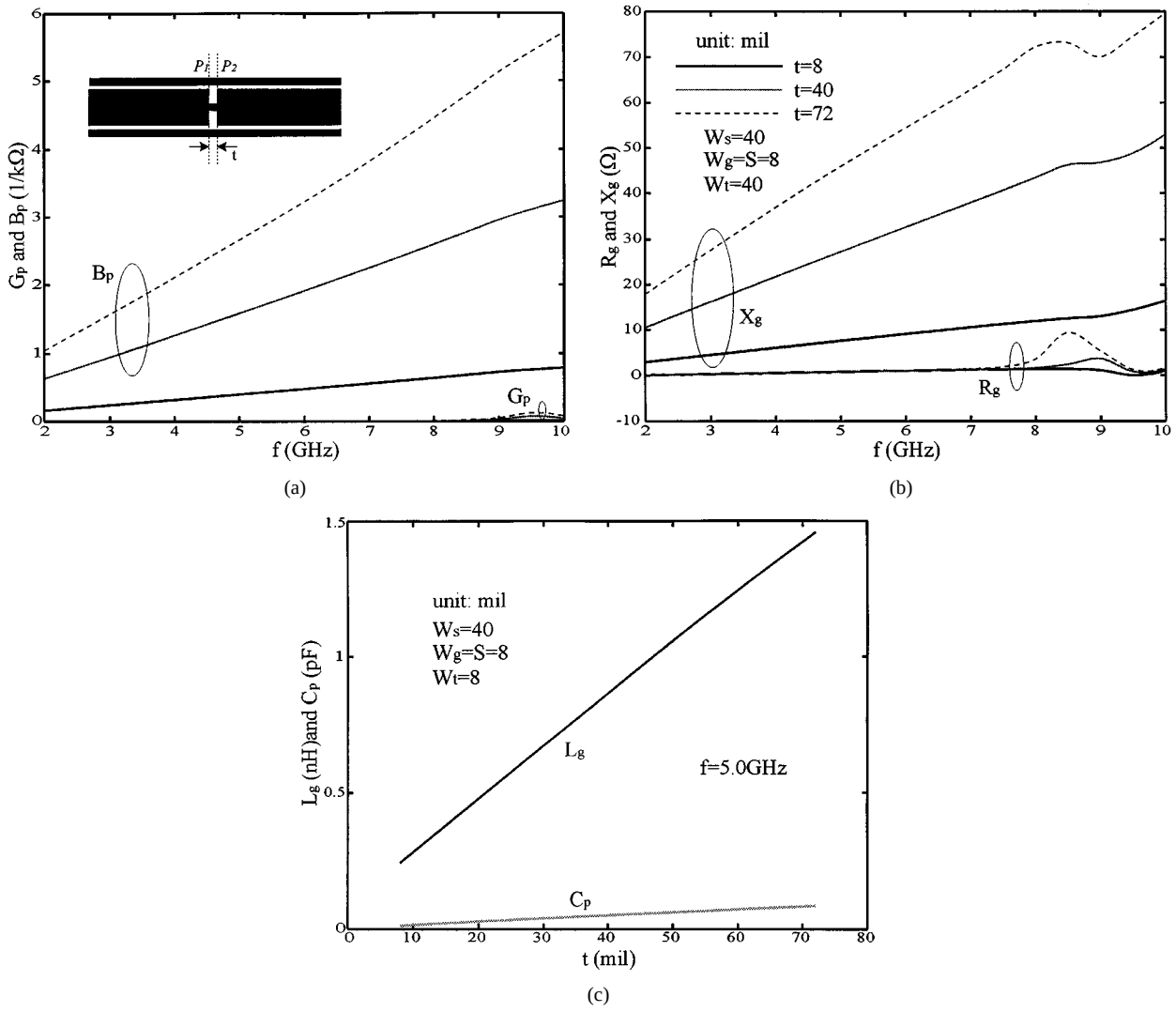

Fig. 9. SOC-calibrated frequency-dependent parametric characteristics of wide-strip FGCPW inductive series-connected elements. (a) Shunt admittance $Y_p = G_p + jB_p$. (b) Series impedance $Z_g = R_g + jX_g$. (c) Lumped shunt capacitance C_p and lumped series inductance L_g.

incrementally at low frequency and then rapidly as frequency increases further as opposed to those of the gap structure. It is attributed to a distributed (parallel) mechanism of coupling. If the IDC finger number is chosen to be large, this structure may be an ideal dc-block circuit in the design of uniplanar active circuits and active antennas [18] in view of its strong capacitive coupling.

B. FGCPW Series Inductance Elements

Fig. 8(a) describes the initial circuit model of the FGCPW inductive series-connected elements, as shown in Fig. 1(c), which consist of two series impedances (Z_a and Z_b) as well as two identical input/output shunt capacitances (C_p). Specifically, Z_a refers to the circuit equivalence of an FGCPW notch line section with narrow width (W_t), including the inductance (L_a) generated by this narrow line and the capacitance (C_a) due to a parasitic coupling between two open ends at the terminals (P_1 and P_2). Z_b is an additional series inductive impedance brought by the other nonnotched finite line section of signal strip or ground strips. Meanwhile, C_p represents the effect of the FGCPW step discontinuity at the planes (P_1 and P_2). Similar to the case of FGCPW capacitive elements, as depicted in Fig. 3, this model can be analytically converted into its more convenient format, as given in Fig. 8(b), by its complete series impedance ($Z_g = Z_a + Z_b$). Note that an additional series inductance (L_b) caused by a finite extent of the FGCPW ground planes is responsible for enhancement of the total series inductance (L_g), which is different from the conventional CPW [1].

Fig. 9(a) and (b) provides the SOC-extracted frequency-dependent circuit parameters versus different length (t) for the FGCPW structure marked by class (A), by transversely notching (or cutting) the signal-strip width. Over the frequency range (2.0–10.0 GHz), the shunt susceptance (B_p) appears to increase quasi-linearly as frequency goes up and its related counterpart (G_p) seems extremely small, as shown in Fig. 9(a). In addition, the series reactance (X_g) seems linearly enhanced as frequency increases up to 8.0 GHz and then to vary slightly in relation with the "resonance" caused by a certain combination of C_a, L_a, and L_b. The series resistance (R_g) is found much small over the wide range, except in the range of "resonance." Due to the reverse orientation of current density flowing along the signal and

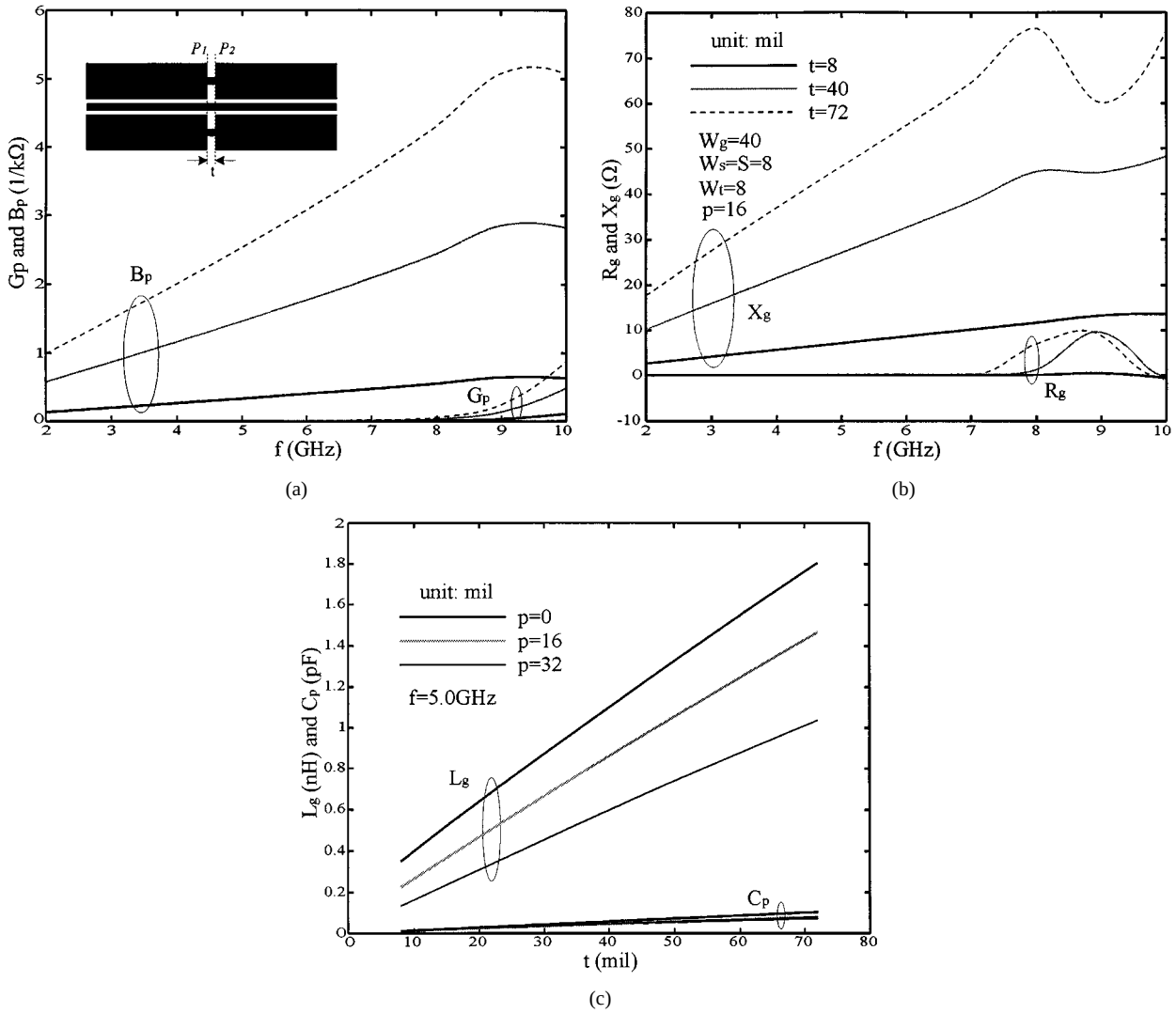

Fig. 10. CAD model-based extracted dispersive circuit parameters of wide-ground FGCPW inductive series-connected elements. (a) Shunt admittance $Y_p = G_p + jB_p$. (b) Series impedance $Z_g = R_g + jX_g$. (c) Lumped shunt capacitance C_p and series inductnace L_g.

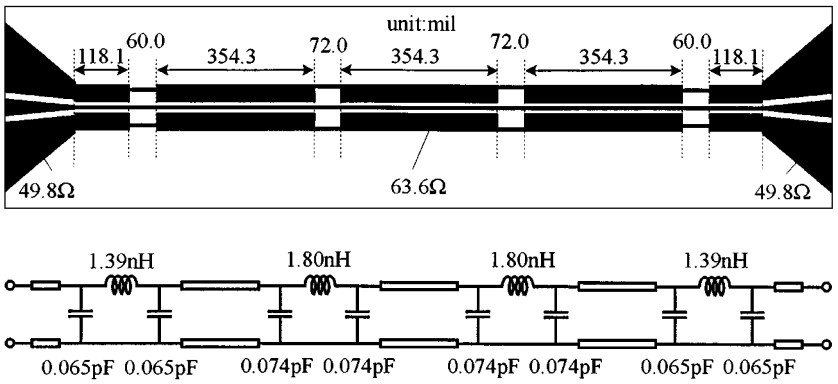

Fig. 11. Detailed physical layout and lumped-element circuit representation of an innovative uniplanar bandstop filter based on the wide-ground FGCPW inductive series-connected elements, as depicted in Fig. 10. This filter is designed to showcase our proposed CAD-oriented unified model based on field theory.

ground strips, the radiation loss is extremely weak compared to the FGCPW gap structures. As the length (t) is extended from 8.0 to 72.0 mil, both L_g and C_p are observed to increase rapidly. Fig. 9(c) gives the extracted L_g and C_p versus the length (t) at a fixed frequency $f = 5.0$ GHz, exhibiting a linear and proportional increase.

Fig. 10(a) and (b) gives a set of curves for the SOC-extracted circuit elements in the case of considering the other FGCPW structure marked by class (B), by transversely notching (or cutting) the two ground strips to build up a pair of narrow line sections at the central location; more precisely, $p = (W_g - W_t)/2$. Very similar electrical properties are observed, and a

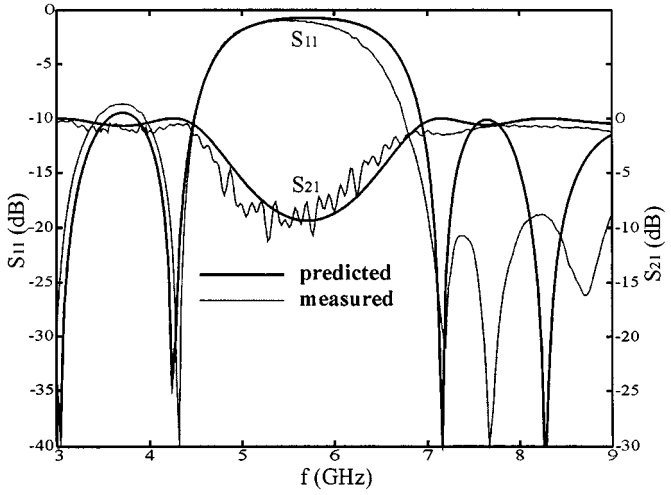

Fig. 12. Predicted and measured return/insertion losses of the proposed three-stage uniplanar bandstop filter (see Fig. 11 for its geometrical design) over the frequency range of 5.8 GHz (industrial–scientific–medical (ISM) band).

quasi-lumped circuit behavior is pronounced at frequency lower than 7.0 GHz for both Z_g and Y_p. Nevertheless, the observed wide-band linear behavior is slightly degraded by and around the "resonance" frequency range for X_g, which is reduced by 1.0 GHz and some "nonlinear" effect for B_p is clearly visible over the range of $f = 8.5 to 10.0$ GHz, especially in the case of $t = 72$ mil. Fig. 10(c) plots the series inductance (L_g) and shunt capacitance (C_p) as a function of the length (t) at frequency $f = 5.0$ GHz for three offset cases ($p = 0, 16$, and 32 mil). Similar linear increment properties versus the notch line length (t) can be well observed for all the three cases, as in Fig. 9(c). As the offset p decreases to move the notch line outwards the signal strip, L_g gains a significant increase, but C_p remains almost unchanged.

C. Innovative Uniplanar Bandstop Filter

With the SOC-extracted circuit model, an innovative filter design example is showcased with theoretical and experimental results for uniplanar FGCPW structures. Fig. 11 shows the layout and its complete equivalent-circuit model of a novel uniplanar multistage bandstop filter, in which each FGCPW line section represents an approximate half-wavelength uniform line resonator at the central frequency (in this paper, $f = 5.8$ GHz). Each FGCPW series element is characterized in terms of a lumped series inductance and a pair of shunt capacitance, which is quantitatively described in Fig. 10. On the basis of the circuit topology, as described in Fig. 11(b), the frequency response of such a filter can be modeled toward its specified electrical performance by applying a circuit network-based optimization procedure [19]. Fig. 12 shows its predicted electrical performance together with our measured results, which exhibit the Chebyshev-type bandstop frequency response. It is found that 3-dB frequency bandwidth with respect to the return loss is wider than 30%, while the insertion loss (S_{21}) outside the stopband range appears to be smoothly varied around the ideal value of 0 dB.

IV. Conclusion

Equivalent-circuit model representation of a large variety of new FGCPW reactive series-connected elements has been extensively investigated in this paper. With the use of our unique SOC scheme self-contained in a full-wave MoM algorithm, extracted parameters of the model can accurately account for various physical effects, including parasitic effects caused by electrically finite ground and/or strip width. Our detailed studies reveal a number of interesting features of the FGCPW structures such as quasi-lumped circuit behavior at low frequency and parasitic lossy "resonance" phenomenon regarding to the radiation effect at high frequency. Those electrical properties including the parasitic effects may be very useful for the design of novel uniplanar and multilayered circuit and antenna building blocks, as the electrical parameters are extracted in a very accurate manner. Our experiments are made to verify the accuracy of our proposed unified circuit model and also observed "resonance" characteristics. With this model, an innovative uniplanar three-stages FGCPW bandstop filter is designed and fabricated on the basis of an efficient circuit network that is extracted from field calculations. It is found that the predicted results are very well compared with our measured frequency response.

References

[1] K. C. Gupta, R. Garg, I. Bahl, and P. Bhartia, "Chapter 7 coplanar lines: Coplanar waveguide and coplanar strips," in *Microstrip Lines and Slotlines*, 2nd ed. Norwood, MA: Artech House, 1996.

[2] G. Ghione and C. Naldi, "Coplanar waveguides for MMIC application: Effect of upper shielding, conductor backing, finite-extent ground planes, and line-to-line coupling," *IEEE Trans. Microwave Theory Tech.*, vol. MTT-35, pp. 260–267, Mar. 1987.

[3] H. Shigesawa, M. Tsuji, and A. A. Oliner, "New interesting leakage behavior on coplanar waveguides of finite and infinite widths," *IEEE Trans. Microwave Theory Tech.*, vol. 39, pp. 2130–2137, Dec. 1991.

[4] N. S. Kuek and S. Uysal, "Investigation of discontinuous coplanar waveguide lines with finite ground planes," in *Proc. Asia–Pacific Microwave Conf.*, Hong Kong, Dec. 1997, pp. 969–972.

[5] F. Brauchler, S. Robertson, J. East, and P. B. Katehi, "W-band finite ground coplanar (FGC) line circuit elements," in *IEEE MTT-S Int. Microwave Symp. Dig.*, June 1996, pp. 1845–1848.

[6] G. E. Ponchak and L. P. Katehi, "Open- and short-circuit terminated series stubs in finite-width coplanar waveguide on silicon," *IEEE Trans. Microwave Theory Tech.*, vol. 45, pp. 970–976, June 1997.

[7] R. W. Jackson, "Considerations in the use of coplanar waveguide for millimeter wave integrated circuits," *IEEE Trans. Microwave Theory Tech.*, vol. MTT-34, pp. 1450–1456, Dec. 1986.

[8] N. I. Dib, L. P. B. Katehi, G. E. Ponchak, and R. N. Simons, "Theoretical and experimental characterization of coplanar waveguide discontinuities for filter application," *IEEE Trans. Microwave Theory Tech.*, vol. 39, pp. 873–882, May 1991.

[9] L. Zhu and K. Wu, "Unified equivalent-circuit model of planar discontinuities suitable for field theory-based CAD and optimization of M(H)MIC's," *IEEE Trans. Microwave Theory Tech.*, vol. 47, pp. 1589–1602, Sept. 1999.

[10] ——, "Network equivalence of port discontinuity related to source plane in a deterministic 3-D method of moments," *IEEE Microwave Guided Wave Lett.*, vol. 8, pp. 130–132, Mar. 1998.

[11] ——, "Revisiting characteristic impedance and its definition of microstrip line with a self-calibration 3D-MoM scheme," *IEEE Microwave Guided Wave Lett.*, vol. 8, pp. 87–89, Feb. 1998.

[12] J. Rautio, "Comments on 'Revisiting characteristic impedance and its definition of microstrip line with a self-calibration 3D-MoM scheme'," *IEEE Microwave Guided Wave Lett.*, vol. 8, pp. 87–89, Feb. 1998.

[13] L. Zhu and K. Wu, "Author's reply," *IEEE Trans. Microwave Theory Tech.*, vol. 47, pp. 115–119, Jan. 1999.

[14] L. Zhu and K. Wu, "Characterization of unbounded multiport microstrip passive circuits using an explicit network-based method of moments," *IEEE Trans. Microwave Theory Tech.*, vol. 45, pp. 2114–2124, Dec. 1997.
[15] R. A. Soares, P. Gouzien, P. Legaud, and G. Follot, "A unified mathematical approach to two-port calibration techniques and some applications," *IEEE Trans. Microwave Theory Tech.*, vol. 37, pp. 1669–1674, Nov. 1989.
[16] D. Rubin, "De-embedding mm-wave MIC's with TRL," *Microwave J.*, pp. 141–150, June 1990.
[17] "Network analysis applying the HP 8510BTRL calibration for non-coaxial measurements," Hewlett-Packard, Santa Rosa, CA, Product Note 8510-8, Oct. 1987.
[18] K. Y. Liu, C. Y. Lee, and T. Itoh, "Non-leaky coplanar waveguide active antenna," in *IEEE MTT-S Int. Microwave Symp. Dig.*, June 1995, pp. 765–767.
[19] G. Matthaei, L. Young, and E. Jones, *Microwave Filters, Impedance-Matching Networks, and Coupling Structures*. Norwood, MA: Artech House, 1980.

Lei Zhu (S'91–M'93–SM'00) was born in Wuxi, Jiangsu Province, China, in 1963. He received the B.Eng. and M.Eng. degrees in radio engineering from the Nanjing Institute of Technology (now Southeast University), Nanjing, Jiangsu, China, in 1985 and 1988, respectively, and the Ph.D.Eng. degree in electronic engineering from the University of Electro-Communications, Tokyo, Japan, in 1993.

From 1985 to 1989, he studied a variety of millimeter-wave passive and active circuits, and leaky-wave antennas using the grooved nonradiative dielectric waveguide (GNRD). From 1989 to 1993, he conducted research on the full-wave characterization and optimization design of planar integrated transmission lines and components. From 1993 to 1996, he was with the Matsushita-Kotobuki Electronics Industries Ltd., Tokyo, Japan, where he was a Research Engineer involved with research and development of planar integrated antenna elements and arrays with compact-size and high-radiation gain/efficiency for application in wireless communications. From 1996 to 2000, he was with the École Polytechnique de Montréal, Montréal, QC, Canada, where he was a Research Fellow. Since July 2000, he has been with the School of Electrical and Electronic Engineering, Nanyang Technological University, Singapore, where he is currently an Associate Professor. His current research works/interests include the study of planar integrated dual-mode filters, ultra-broad-bandpass filters, broad-band interconnects, planar antenna elements/arrays, uniplanar CPW/CPS circuits, as well as full-wave 3-D method-of-moments (MoM) modeling of planar integrated circuits and antennas, numerical deembedding or parameter-extraction techniques, and field-theory-based CAD synthesis/optimization design procedures.

Dr. Zhu was the recipient of the Japanese Government (Monbusho) Graduate Fellowship (1989–1993). He was also the recipient of the 1993 First-Order Achievement Award in Science and Technology presented by the National Education Committee, China, the 1996 Silver Award of Excellent Invention presented by the Matsushita-Kotobuki Electronics Industries Ltd., Japan, and the 1997 Asia–Pacific Microwave Prize Award presented at the Asia–Pacific Microwave Conference, Hong Kong.

Ke Wu (M'87–SM'92–F'01) was born in Liyang, Jiangsu Province, China. He received the B.Sc. degree in radio engineering (with distinction) from the Nanjing Institute of Technology (now Southeast University), Nanjing, China, in 1982, and the D.E.A. and Ph.D. degrees in optics, optoelectronics, and microwave engineering (with distinction) from the Institut National Polytechnique de Grenoble (INPG), Grenoble, France, in 1984 and 1987, respectively.

He conducted research in the Laboratoire d'Electromagnetisme, Microondes et Optoelectronics (LEMO), Grenoble, France, prior to joining the Department of Electrical and Computer Engineering, University of Victoria, Victoria, BC, Canada. He subsequently joined the Department of Electrical and Computer Engineering, École Polytechnique de Montréal, Montréal, QC, Canada, as an Assistant Professor, and is currently a Full Professor. He has held visiting or guest professorships at Telecom-Paris, Paris, France, and INP-Grenoble, Grenoble, France, the City University of Hong Kong, the Swiss Federal Institute of Technology (ETH-Zurich), Zurich, Switzerland, the National University of Singapore, Singapore, the University of Ulm, Ulm, Germany, as well as many short-term visiting professorships at other universities. He also holds an Honorary Visiting Professorship at the Southeast University, China. He has been the Head of the FCAR Research Group of Quebec on RF and microwave electronics, and the Director of the Poly-Grames Research Center, as well as the Founding Director of the newly developed Canadian Facility for Advanced Millimeter-wave Engineering (FAME). He has authored or co-authored over 300 referred journal and conference papers, and also several book chapters. His current research interests involve 3-D hybrid/monolithic planar and nonplanar integration techniques, active and passive circuits, antenna arrays, advanced field-theory-based CAD and modeling techniques, and development of low-cost RF and millimeter-wave transceivers. He is also interested in the modeling and design of microwave photonic circuits and systems. He is an Editorial Board member for *Microwave and Optical Technology Letters*.

Dr. Wu is a member of the Electromagnetics Academy. He was chairperson of the 1996 Symposium on Antenna Technology and Applied Electromagnetics (ANTEM) Publicity Committee and vice-chairperson of the Technical Program Committee (TPC) for the 1997 Asia–Pacific Microwave Conference (APMC'97). He has served on the FCAR Grant Selection Committee and the TPC committee for the International Conference on Telecommunications in Modern Satellite Cable and Broadcasting Services (TELSIKS) and International Microwave and Optical Technology (ISMOT). He has also served on the ISMOT International Advisory Committee. He was the general co-chair of the 1999 and 2000 SPIE International Symposium on Terahertz and Gigahertz Electronics and Photonics, Denver, CO, and San Diego, CA, respectively. He was the general chair of the 8th International Microwave and Optical Technology (ISMOT'2001), Montreál, QC, Canada, June 19–23, 2001. He has served on the Editorial or Review Boards of various technical journals, including the IEEE TRANSACTIONS ON MICROWAVE THEORY AND TECHNIQUES, the IEEE TRANSACTIONS ON ANTENNAS AND PROPAGATION, and the IEEE MICROWAVE AND GUIDED WAVE LETTERS He served on the 1996 IEEE Admission and Advancement (A&A) Committee, the Steering Committee for the 1997 joint IEEE Antennas and Propagation Society (IEEE AP-S)/URSI International Symposium. He has also served as a TPC member for the IEEE Microwave Theory and Techniques Society (IEEE MTT-S) International Microwave Symposium. He was elected to the Board of Directors of the Canadian Institute for Telecommunication Research (CITR). He also serves on the Technical Advisory Board of Lumenon Lightwave Technology Inc. He is currently the chair of the joint IEEE chapters of the IEEE MTT-S/IEEE AP-S/IEEE Lasers and Electro-Optics Society (IEEE LEOS), Montreál, QC, Canada. He was the recipient of the URSI Young Scientist Award, the Institute of Electrical Engineers (IEE), U.K., Oliver Lodge Premium Award, the Asia–Pacific Microwave Prize Award, the University Research Award "Prix Poly 1873 pour l'Excellence en Recherche" presented by the École Polytechnique on the occasion of its 125th anniversary, and the Urgel–Archambault Prize (the highest honor) in the field of physical sciences, mathematics and engineering presented by the French–Canadian Association for the Advancement of Science (ACFAS).